Chaotic Modeling and Simulation (CMSIM) **1: 55-73, 2020**

Investigation of chaotic dynamics of Chua's circuit implemented by means of the matrix decomposition method

Alexander M. Krot[1], Uladzislau A. Sychou[2]

[1] United Institute of Informatics Problems of National Academy of Sciences of Belarus, Laboratory of Self-Organization System Modeling, Minsk, Belarus
(E-mail: alxkrot@newman.bas-net.by)
[2] United Institute of Informatics Problems of National Academy of Sciences of Belarus, Laboratory of Robotic Systems, Minsk, Belarus
(E-mail: vsychyov@robotics.by)

Abstract: A number of works devoted to chaotic dynamics in electronic circuits grows every year. An important task in this analysis is to identify chaotic states in a circuit or to purposefully excite chaotic oscillations. The scope of this study is to analyze Chua's circuit with a cubic nonlinearity using Krot's method of matrix decomposition into a state-space. In this method, the system of Chua's nonlinear equations is expanded into a matrix series. As a result, linear, cubic and quadratic matrix terms are obtained. Numerical integration of these matrix terms makes it possible to estimate the influence of higher-order nonlinearities on the Chua's circuit chaotic regime as well as to observe a chaotic attractor that restoring based on the linear, quadratic and cubic matrix terms. The study has been carried out using the Simulink-model, which can be implemented in embedded systems as a generator of chaotic signals. It is shown that the regime of hard self-excited oscillations leads to appear a double scroll chaotic attractor in the state-space.
Keywords: Nonlinear dynamical system, Chua's circuit, chaotic double-scroll attractor, matrix decomposition method, hard self-excited oscillations

1 Introduction

Chua's circuit is one of the most studied chaotic generators. There is the number of researches devoted to the usage of this circuit as a physical device in "reservoir computing" approach or as an element of associative memory [1], however, for recording/decoding the output signals from Chua's scheme just great resources are needed. The method for analysis of attractors of complex nonlinear dynamical systems (NDS) has been developed based on Krot's decomposition matrix series into a state-space (a phase space) [2-9]. This paper shows that the matrix decomposition method can be used to analyze of Chua's circuit as well.

Received: 9 January 2020 / Accepted: 30 January 2020

ISSN 2241-0503

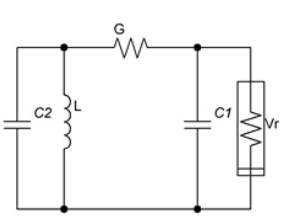

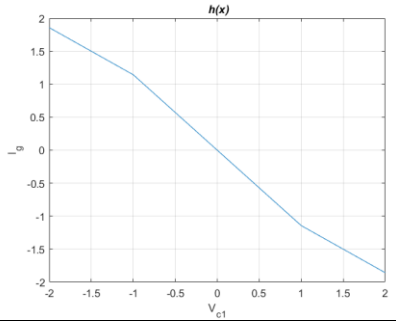

a) b)

Figure 1 – Chua's circuit (a) and piece-wise linear characteristic (b) of the Chua's nonlinear element V_r

Let us consider Chua's circuit (see Fig. 1a) and the system of equations describing the circuit (which obtained using Kirchhoff's circuit laws in the paper [10]):

$$\begin{aligned} \frac{dx}{dt} &= \alpha(y - x - h(x)) \\ \frac{dy}{dt} &= x - y + z \\ \frac{dz}{dt} &= -\beta y \end{aligned} \tag{1}$$

$$h(x) = m_1 x + \frac{1}{2}(m_0 - m_1)(|x+1| - |x-1|). \tag{2}$$

As known [10], chaotic dynamics can be observed when:

$$\alpha = 15.6; \beta = 28; m_0 = -1.143; m_1 = -0.714; \tag{3}$$

The plot of the piecewise function $h(x)$ is shown in Fig. 1b. This nonlinearity is commonly used in computer simulations of Chua's circuit, but it is difficult to implement on real-world hardware as well as to analyze using the matrix decomposition method. That is why we have to use a smooth nonlinearity like the one described in [11-16].

In this work, the cube polynomial

$$p(x) = Ax^3 + Bx^2 + Cx + D \tag{4}$$

is chosen as a nonlinear function to approximate the function $h(x)$.

Here coefficients A, B, C, D can be found to approximate the curve shown in Fig. 1b. For good approximation four points are needed (see Table 1):

Table 1 – The points are chosen to approximate the nonlinear function $h(x)$

№	X (V_{c1})	Y(I_g)
1	-1	1.143
2	0	0
3	1	-1.143
4	2	-1.857

$$\begin{bmatrix} A \\ B \\ C \\ D \end{bmatrix} = \begin{bmatrix} X_1^3 & X_1^2 & X_1^1 & X_1^0 \\ X_2^3 & X_2^2 & X_2^1 & X_2^0 \\ X_3^3 & X_3^2 & X_3^1 & X_3^0 \\ X_4^3 & X_4^2 & X_4^1 & X_4^0 \end{bmatrix}^{-1} \begin{bmatrix} Y_1 \\ Y_2 \\ Y_3 \\ Y_4 \end{bmatrix} = \begin{bmatrix} -1 & 1 & -1 & 1 \\ 0 & 0 & 0 & 1 \\ 1 & 1 & 1 & 1 \\ 8 & 4 & 2 & 1 \end{bmatrix}^{-1} \begin{bmatrix} 1.143 \\ 0 \\ -1.143 \\ -1.857 \end{bmatrix} = \begin{bmatrix} 0.0715 \\ 0 \\ -1.2145 \\ 0 \end{bmatrix} \quad (5)$$

As can be seen from Eq. (5), only coefficients A and C of the polynomial (4) are non-zero. Substituting $p(x)$ into (1) instead $h(x)$ (2) we obtain the system of equations:

$$\begin{cases} \dot{u}_1 = \alpha u_2 - A\alpha u_1^3 - C\alpha u_1 \\ \dot{u}_2 = u_1 - u_2 + u_3 \\ \dot{u}_3 = -\beta u_2 \end{cases} \quad (6)$$

where α, β are control parameters, u_1, u_2, u_3 are variables in the state space of Chua's circuit.

To use Krot's method of matrix decomposition for analysis of Eqs. (6) the system of equations has to be rewritten in matrix notation:

$$\dot{\vec{u}} = \vec{f}(\vec{u}, \alpha, \beta, A, C) \ , \quad (7a)$$

where

$$\dot{\vec{u}} = \begin{bmatrix} \dot{u}_1 \\ \dot{u}_2 \\ \dot{u}_3 \end{bmatrix}; \qquad \vec{f} = \begin{bmatrix} \alpha u_2 - A\alpha u_1^3 - C\alpha u_1 \\ u_1 - u_2 + u_3 \\ -\beta u_2 \end{bmatrix}. \quad (7b)$$

The dependence of the vector function $\vec{f}$ on the variables $u_i = u_i^* + v_i, i = 1,2,3$ has been considered in [4]. This dependence is true under the condition of the influence of small perturbations v_i when $|v_i| \ll |u_i|$. Taking into account the mention above, we can see that the change of vector function (7b) is the following:

$$\Delta \dot{\vec{u}} = \Delta \vec{f}(\vec{v}, \vec{u}^*, \alpha, \beta, A, C) \quad (8a)$$

where

$$\Delta\vec{f}(\vec{v},\vec{u}^{\,*},\alpha,\beta,A,C)=\vec{f}(\vec{u}^{\,*}+\vec{v},\alpha,\beta,A,C)-\vec{f}(\vec{u}^{\,*},\alpha,\beta,A,C)=$$

$$=\begin{bmatrix}\alpha u_2^*+\alpha v_2-A\alpha(u_1^*+v_1)^3-C\alpha u_1^*-C\alpha v_1\\ u_1^*+v_1-u_2^*-v_2+u_3^*+v_3\\ -\beta u_2^*-\beta v_2\end{bmatrix}-$$

$$-\begin{bmatrix}\alpha u_2^*-A\alpha u_1^{*3}-C\alpha u_1^*\\ u_1^*-u_2^*+u_3^*\\ -\beta u_2^*\end{bmatrix}=\begin{bmatrix}\alpha v_2-A\alpha(u_1^*+v_1)^3-C\alpha v_1+A\alpha u_1^{*3}\\ v_1-v_2+v_3\\ -\beta v_2\end{bmatrix}= \tag{8b}$$

$$=\begin{bmatrix}\alpha v_2-(3A\alpha u_1^{*2}+C\alpha)v_1-3A\alpha u_1^* v_1^2-A\alpha v_1^3\\ v_1-v_2+v_3\\ -\beta v_2\end{bmatrix}$$

The change of the vector function can be fully described by means of linear, quadratic and cubic terms of matrix series [2]-[7]:

$$\Delta\vec{f}(\vec{v},\vec{u}^{\,*})=L_{3x3}^{(1)}\vec{v}+\frac{1}{2!}L_{3x9}^{(2)}(\vec{v}\otimes\vec{v})+\frac{1}{3!}L_{3\times27}^{(3)}(\vec{u}^{\,*})(\vec{v}\otimes\vec{v}\otimes\vec{v}), \tag{9}$$

where $L_{3\times3}^{(1)}$, $L_{3\times9}^{(2)}$, $L_{3\times27}^{(3)}$ are matrix terms of the following form:

$$L_{3x3}^{(1)}=\begin{bmatrix}-(3A\alpha u_1^{*2}+C\alpha) & \alpha & 0\\ 1 & -1 & 1\\ 0 & -\beta & 0\end{bmatrix}; \tag{10}$$

$$L_{3x9}^{(2)}==\begin{bmatrix}-6A\alpha u_1^* & 0 & 0 & 0 & 0 & 0 & 0 & 0 & 0\\ 0 & 0 & 0 & 0 & 0 & 0 & 0 & 0 & 0\\ 0 & 0 & 0 & 0 & 0 & 0 & 0 & 0 & 0\end{bmatrix}; \tag{11}$$

$$L_{3\times27}^{(3)}(\vec{u}^{\,*})=\begin{bmatrix}-6A\alpha & 000000000000000000000000000\\ 0 & 000000000000000000000000000\\ 0 & 000000000000000000000000000\end{bmatrix}. \tag{12}$$

and $\overbrace{\vec{v}\otimes\vec{v}\otimes\ldots\otimes\vec{v}}^{k}$ is the Kronecker's k^{th} degree of a vector $\vec{v}$, k =1,2,3, for example, $\vec{v}\otimes\vec{v}=[v_1^2\ v_1v_2\ v_1v_3\ldots v_3^2]^T$.

Computations based on the matrix decomposition (9)-(12) show that

$$\Delta\vec{f}=\begin{bmatrix}-(3A\alpha u_1^{*2}+C\alpha)v_1+\alpha v_2\\ v_1-v_2+v_3\\ -\beta v_2\end{bmatrix}+\frac{1}{2}\begin{bmatrix}-6A\alpha u_1^* v_1^2\\ 0\\ 0\end{bmatrix}+\frac{1}{6}\begin{bmatrix}-6A\alpha v_1^3\\ 0\\ 0\end{bmatrix} \tag{13}$$

In equation (13), the variables of the system are v_1, v_2, v_3, and the parameters are α, β, A, C, as well as the stationary value u_1^* of the first variable u_1 can be also considered as a parameter.
Using the above results we are going to look at the processes leading to chaos states in the circuit with the aim to find conditions of chaos origin.

2 Synthesis and analysis of the Chua's circuit computational model based on the matrix decomposition method.

Considerable attention is given to developing new methods for analyzing electronic circuits. The primary goal of the matrix decomposition method is to apply nonlinear analysis for estimating the influence of terms $L^{(1)}_{N\times N}$, $L^{(2)}_{N\times N^2}$, $L^{(3)}_{N\times N^3}$ … on circuit dynamics [2-7]. It allows us to use the matrix decomposition method as a base of the computational model to study the Chua's system. For this purpose, let us look into Simulink-model (Figure 2) based on the system of equations (13) with the usage of the matrix decomposition method.

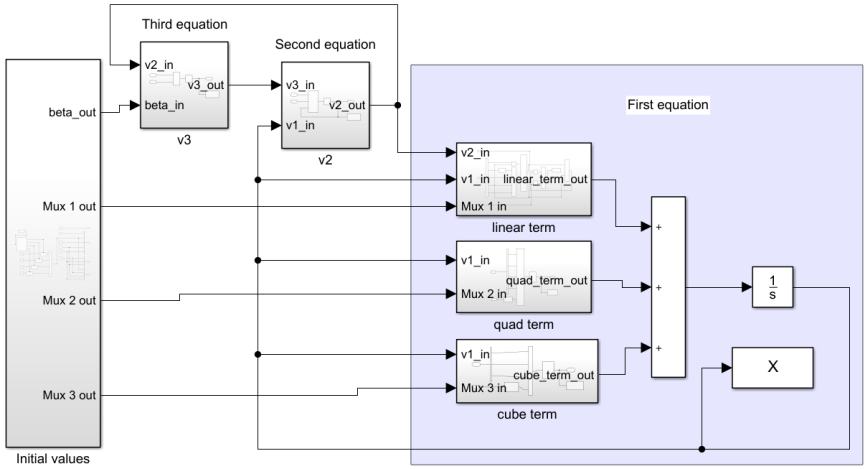

Figure 2 – Simulink-model's main blocks that represent three equations of system (13) based on the matrix decomposition and definition of initial values

The computational model is consisting of several subsystems: initial values subsystem, subsystems for computation of values v_2, v_3 (second equation and third equation respectively), subsystems for computation of linear, quadratic and cubic terms of the matrix series. The latter subsystems are grouped under first equation label for computation of v_1 . The basic blocks of Simulink such as multipliers or integrators are used as well.

According to Eq. (5) the coefficients of the polynomial (4) have been found, moreover, $B = D = 0$. However, the obtained set of coefficients is not only one possible set. Further smoothing of nonlinearity is allowed without losing of chaotic oscillations. Moreover, there exists a state in which chaotic oscillations can be observed under a wide range of values u_1^*. For example, one possible set has been found during a number of simulations, when $A = 0.002$, $C = -1.3$, $\beta = 28$, $\alpha = 15.6$. In this section, we investigate both sets of coefficients and influence of the value u_1^* on the system dynamics (see Table 2).

Table 2 The studied sets of parameters

No.	A	C	u_1^*
1	0.002	-1.3	-0.75 (chosen from Fig. 3)
2	0.0715	-1.2145	-0.05 (chosen from Fig. 4)

Figures 3 and 4 show dependence v_1 on u_1^*. As a result of multiple simulations, each column of circles is a one-dimensional representation of two-dimensional attractor. As can be seen in Fig. 3, a chaotic state is observed on a wide range of values u_1^*. For comparison, the second case (see Table 2 as well as Fig. 4), demonstrates the chaotic regime only in a narrow interval near the small value u_1^* .

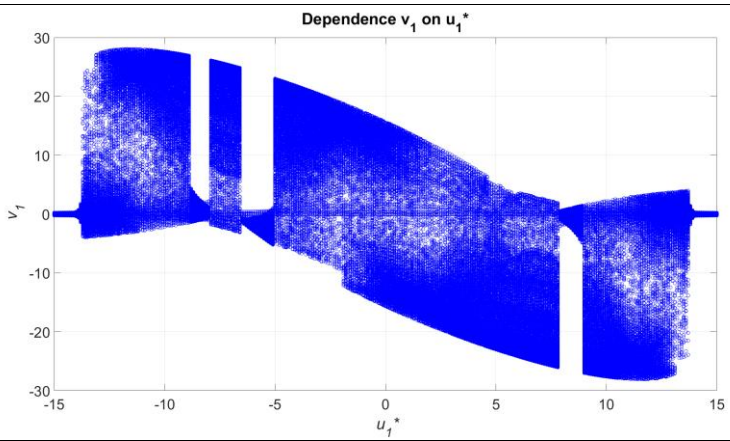

Figure 3 – The dependence of v_1 on u_1^* for $A = 0.002$ and $C = -1.3$ shows that chaotic behaviour exists under the wide interval near the values u_1^*

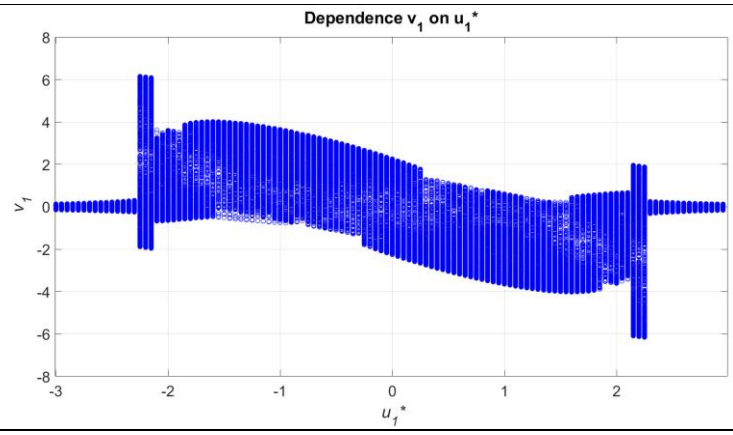

Figure 4 – The dependence of v_1 on u_1^* for $A = 0.0715$ and $C = -1.2145$ shows that chaotic behaviour exists only near the narrow region $|u_1^*| < 2.3$.

Fig. 5 shows phase trajectories in the state space (v_1, v_2, v_3) for both sets of parameters. The Chua's attractor (also called the "double scroll" attractor) is observed in both cases. The simulation shows the significant influence of value u_1^* on the dynamics of Chua's circuit built with the usage of the matrix decomposition method.

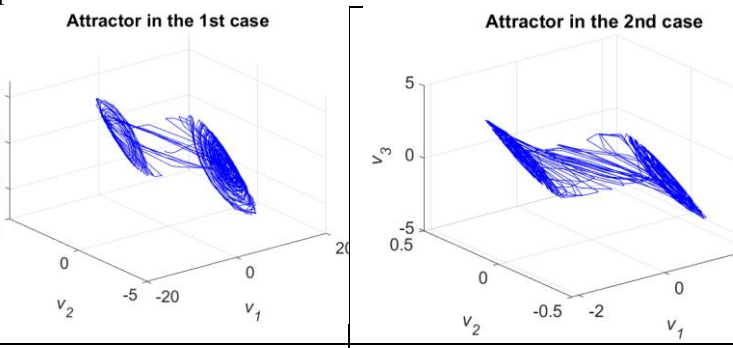

a) b)

Figure 5 – Variants of chaotic attractors in the first (a) and the second (b) cases (see Table 2) showing similar shapes and significant difference in amplitudes

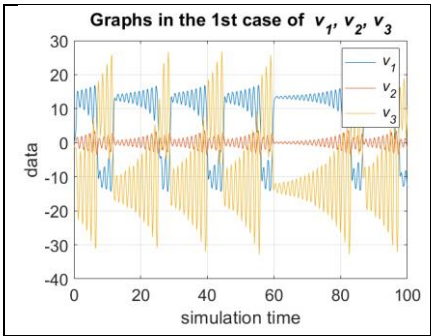

a)

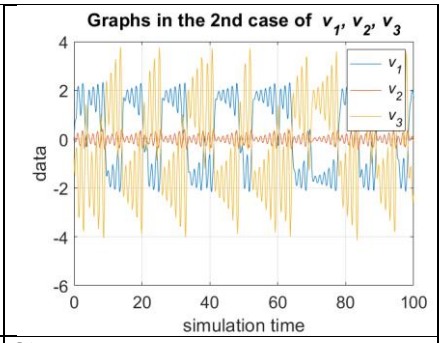

b)

Figure 6 – Dependences of variables v_1, v_2, v_3 on simulation time in the first (a) and the second (b) cases (see Table 2) showing the influence of the degree of nonlinearity as well as value u_1^* on the amplitude and the frequency of chaotic oscillations

The described results show that application of the matrix decomposition method [2]-[7] for analysis of nonlinear electronic circuits like the Chua's circuit allows getting new data about the dynamics of such systems. Moreover, this method makes it possible to estimate the influence of high order nonlinearities on a chaotic regime of circuits.

The matrix decomposition method allows us to introduce a new parameter u_1^* influencing on system dynamics. It can be used for purposeful control of the system in applied tasks like reservoir computing [1] or cryptography.

3 Spectrum analysis of chaotic oscillations in Chua's electronic circuit in the context of Landau's initial turbulence model and theory of Ruelle-Takens

Like other generators, Chua's circuit can generate oscillations with some frequency ω under a wide range of parameters. However, finite continuous chaotic oscillations can be observed only with a specific balance of contributions of the linear $L^{(1)}_{N\times N}$, quadratic $L^{(2)}_{N\times N^2}$ and cubic $L^{(3)}_{N\times N^3}$ kernels of Krot's matrix series into a whole system dynamics. The process of transition from periodic

oscillations with a single frequency to chaotic ones can be explained in full accordance with Landau's initial turbulence model [17].

Using the matrix decomposition method (9)-(13) with regard to Eq. (8a), (8b) let us rewrite an equation for change v_1 of the first component u_1 of the vector variable $\vec{u}$ in the Chua's circuit state space:

$$\dot{v}_1 = c(v_2) + \gamma_L v_1 - \alpha_L v_1^2 - \beta_L v_1^3, \tag{14a}$$

where coefficients are

$$c(v_2) = \alpha v_2;\ \gamma_L = -C\alpha - 3A\alpha u_1^{*2};\ \alpha_L = 3A\alpha u_1^{*};\ \beta_L = 3A\alpha. \tag{14b}$$

Considered parameters are $A = 0.002$, $C = -1.3$, $\beta = 28$, $\alpha = 15.6$ and $u_1^{*} = -0.75$ give us the following inequalities:

$$\gamma_L = -\alpha(3Au_1^{*2} + C) > 0; \tag{15a}$$

$$\alpha_L = 3A\alpha u_1^{*} < 0; \tag{15b}$$

$$\beta_L = A\alpha > 0, \tag{15c}$$

The obtained conditions (15a-c) fully coincide with conditions for *hard self-excited oscillations* within the framework of Landau's initial turbulence model [17]. It means that after the breakdown of the steady-state regime of fluid flow the same inequality (15a) is valid as well as Eq. (14a) is true up to third-order terms where γ_L is a decay factor, α_L is a Landau constant, β_L is a positive (or negative) constant. It should be mentioned that for the *hard self-excited oscillations* β_L must be only a positive constant. In accordance with Landau's model [17] proposed in 1944, a jump-like transition from the stationary regime of a nonlinear system to the nonstationary one leads to appear two extra frequencies ω_1 and ω_2. These frequencies define two cycles (double scroll) in the state-space of Chua's circuit (see Fig. 5a, b).

The results can be explained from the point of view of the Ruelle-Takens approach [18]. This theory was proposed in 1972 and developed in 1978 by Ruelle, Takens, and Newhouse (RTN theory) [19]. The RTN theory has significant scientific and historical value because for the first time it answered the question on Landau's mechanism of turbulence arising [17]. According to Landau's mechanism, an infinite number of Hopf bifurcations is required for turbulence origin [20]. Unlike the Landau's model, within the framework of RTN theory, a small number of bifurcations is required for origin of the chaotic regime [19],[20].

Let us consider a dynamical system in stationary regime, for example, a laminar viscous flow within the framework of Landau's model of initial turbulence. Let us suppose that under increasing the control parameter (the Reynolds number for a viscous flow) the stationary regime is losing stability and leads to the periodical

regime with oscillation mode. In this regime, the frequency ω_1 appears. The plot of the corresponding finite cycle in the state-space is shown in Fig. 7. Next, let us suppose that the same process can be repeated twice. As a result, three Hopf bifurcations could take place and three independent frequencies ω_1, ω_2 and ω_3 could arise. It means that the quasiperiodic mode with three frequencies is realized in the system.

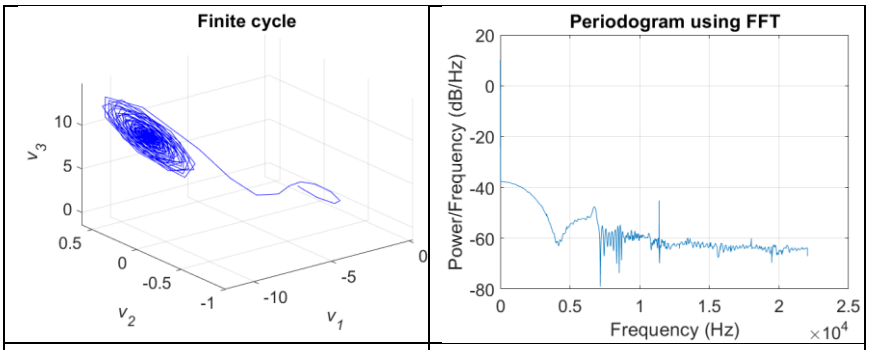

a) b)

Figure 7 – Finite cycle in the state space (a) and periodogram of the signal v_1 (b) showing a peak at 11 390 Hz, -45.17 dB

In the state-space of a system, in accordance with Landau's model of initial turbulence [17], a two-dimension attractor of the kind "torus" T^2 corresponds to a quasi-periodic regime with two independent frequencies as well as a three-dimension attractor torus T^3 corresponds to a quasi-periodic regime with three frequencies [19].

However, unlike the Landau's model of initial turbulence, Ruelle, Takens and Newhouse showed that some disturbances could destroy the torus T^3 and transform it into a chaotic (strange) attractor. It means that the non-stationary behaviour of a system (quasiperiodic regime with three frequencies) ceases to be stable and it becomes chaotic one. However, unlike the torus T^3 a chaotic attractor is stable against disturbances acting on the system [19,20].

Therefore, according to the RTN theory, the power spectrum of a signal from the dynamical system representing the Chua's circuit as a function of the control parameter (Fig. 8) is evolving as follows. After the first Hopf bifurcation, the power spectrum contains one frequency, then after the second Hopf bifurcation, two frequencies arise. Sometimes, if the third Hopf bifurcation occurs then the power spectrum contains three frequencies. However, the third frequency may

not be detected before chaos is identified in the circuit [20]. As soon as the third frequency appears in the power spectrum, a noise component appears, too. This noise component is a feature characterizing the chaos.

Let us consider previous statements on the simulation that implements the spectral analysis of chaotic oscillations in the Chua's circuit. Figure 8 shows the bifurcation diagram, i.e. the dependence of the value of v_1 on the control parameter α.

To determine the values of α and β, ratios of capacitance and inductance in the real-world Chua's circuit can be used, as shown in [10]. As a result, the chaotic mode is observed when $\alpha = 15.6$ and $\beta = 28$.

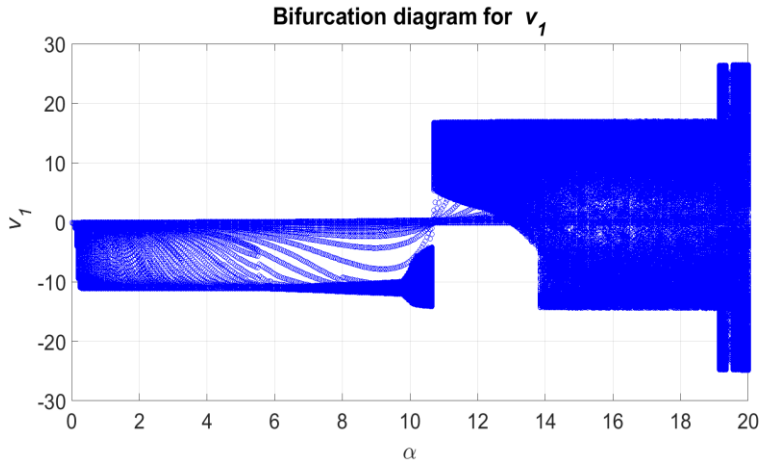

Figure 8 – Bifurcation diagram illustrating the dependence of the value v_1 on the control parameter α.

The computer simulation realized by means of the matrix decomposition method finds that the "double scroll" (which is defined by the two cycles with the frequencies ω_1 and ω_2) is observed in Chua's circuit. It starts approximately with $\alpha = 13.8$ up to $\alpha = 19.0$ (Fig. 8). The figures below (Fig. 9) show the dependence of the power spectra of one of the state-space variables v_1 on the control parameter α. Table 3 contains data on the magnitude and frequency of the resulting spectral modes (peaks) depending on various values α. The data obtained on three thousand iterations with $u_1^* = -0.75$.

Table 3. Parameters of the peaks on spectrogram.

$\alpha=9.75$ (fig.6a)		$\alpha=10$ (fig. 6b)		$\alpha=11.5$ (fig. 6c)		$\alpha=12.3$ (fig. 6d)		$\alpha=13.5$ (fig. 6d)		$\alpha=14$ (fig. 6e)	
Hz	dB	Hz	dB	Hz	dB	Hz	dB	Hz	dB	Hz	dB
1763	-39.4	1769	-33.7	409.5	-40.4	196	-36.6	447.7	-27.3	3585	-15.2
5899	-23.2	3777	-36.6	767.8	-37.6	392	-40.3	597	-25.4	4581	-17.0
13520	-46.7	5581	-09.4	1177	-32.4	710.5	-38.9	920	-21.0	7625	-27.3
		7350	-34.2	1561	-24.9	1397	-34.0	1592	-21.7	14000	-40.1
		9119	-36.1	1945	-34.0	1593	-30.2	3084	-17.8		
		11130	-27.5	2329	-29.1	2107	-35.0	3855	-13.7		
		12930	-32.2	3481	-29.8	2499	-30.6	4104	-41.0		
		14700	-52.9	3890	-22.2	4116	-05.6	8109	-24.4		
		16470	-37.3	4326	-06.3	8208	-22.0	9477	-32.1		
		18480	-45.0	8625	-17.5	12620	-33.8	12060	-35.4		
		20280	-35.6	12900	-31.4	16880	-43.0				
						19400	-40.3				

The attractors corresponding to the periodograms in Fig. 9 are shown in Fig. 10. Plots 9 and 10 confirm that the first bifurcation leads to transition from the initial steady-state (fixed point) to a periodic state (limit cycle) in the phase state-space of Chua's circuit, and the Hopf second bifurcation transforms the periodic regime (with frequency ω_1) to a quasi-periodic regime (with the frequencies ω_1 and ω_2).

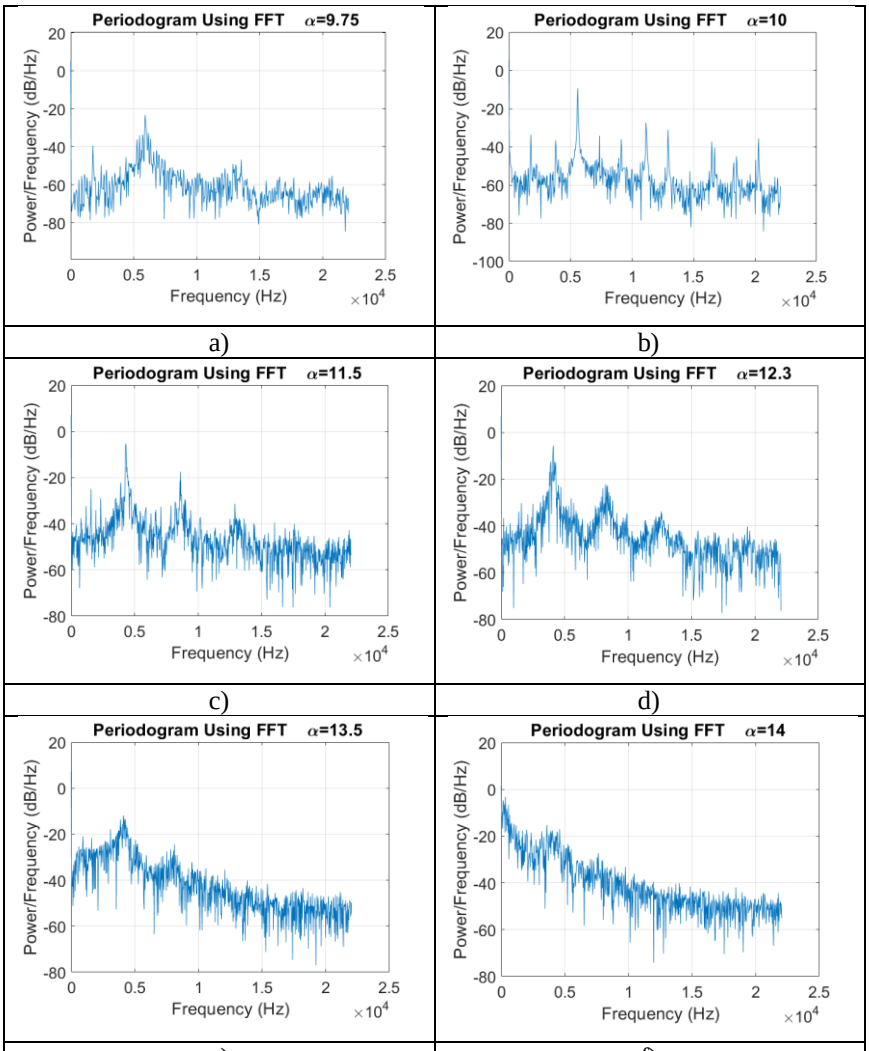

Figure 9 – Periodograms based on FFT of the signal v_1 for the different values of α (Table 2, No. 1): a) $\alpha = 9.75$; b) $\alpha = 10$; c) $\alpha = 11.5$; d) $\alpha = 12.3$; e) $\alpha = 13.5$; f) $\alpha = 14$.

It is well-known [20] that the function x (depends on variables $t_1, t_2, ..., t_r$) is called periodical one with the period 2π for each of the arguments if the value of function does not change when increasing any of the variables by 2π:

$$x(t_1, t_2 ..., t_j, ..., t_r) = x(t_1, t_2 ..., t_j + 2\pi, ...t_r), \; j = 1, 2, ...r \,. \qquad (16)$$

Such function is called quasi-periodic in time if all r variables are proportional to time t:

$$t_j = \omega_j t, \; j = 1, ..., r. \qquad (17)$$

Obviously, the quasiperiodic function has r fundamental frequencies ω_j and, therefore, r periods: $T_j = \dfrac{2\pi}{\omega_j}$, $\quad j = 1, ..., r$ (Fig. 9f).

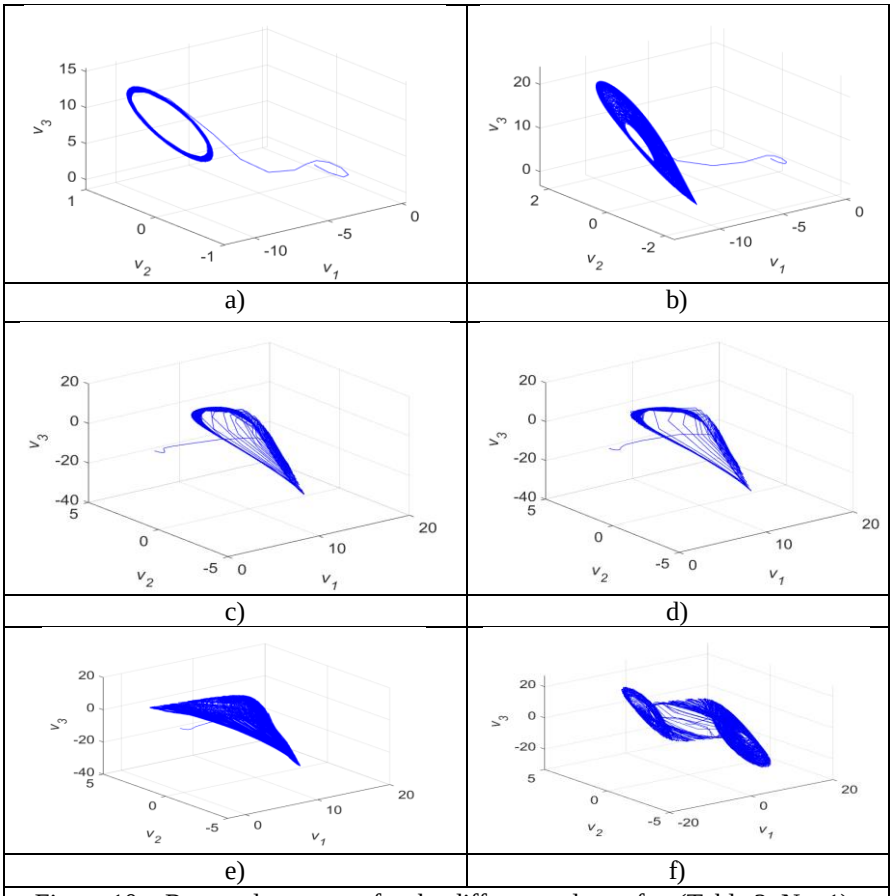

Figure 10 – Restored attractors for the different values of α (Table 2, No. 1): a) $\alpha = 9.75$; b) $\alpha = 10$; c) $\alpha = 11.5$; d) $\alpha = 12.3$; e) $\alpha = 13.5$; f) $\alpha = 14$.

Taking into account the provisions of the RTN theory [18], let us consider the simplest case when $r=2$. According to the number theory, under the condition of irrational ration ω_1/ω_2, any real number is arbitrarily close to one of the sums $|m_1\omega_1+m_2\omega_2|$. Consequently, the power spectrum of a quasi-periodic signal with two periods (the corresponding attractor is a two-dimensional torus T^2 within the framework of the RTN theory) is also dense everywhere. However, this does not mean that the spectrum can be represented by a continuous function since it would correspond to the case of an aperiodic signal. Indeed, two peaks (reasonably close to each other on the frequency axis) should not necessarily have close amplitudes (Fig. 9a-f).

To clarify all the features of the quasi-periodic signal power spectrum with two frequencies ω_1 and ω_2 we use the results of the simulation presented in Table 3. The power spectrum of such a quasi-periodic signal is usually identified using two fundamental frequencies ω_1 and ω_2 which would allow representing the frequencies of modes with large amplitude in the form of simple combinations $|m_1\omega_1+m_2\omega_2|$ with small values of m_1 and $m_2=0,\pm1,\pm2,...$ (Fig. 9*a*).

The first column of Table 3 and Figure 9a show that the spectral peaks on the frequencies 1763 Hz, 5899 Hz and 13520 Hz could be modes with harmonics which are multiples of the fundamental frequency $\omega_1=1763$ Hz with the multipliers $m_1=3$ and $m_2=7$ respectively. At the same time, spectral "troughs" (not presented in Table 3) at the frequencies 1547 Hz, 7 410 Hz, and 14 890 Hz and others correspond to the “missing modes” at multiple harmonics of the fundamental frequency 1547 Hz. Thus, the power spectrum is lined at the value of the control parameter $\alpha=9.75$, as can be seen in Figure 9a.

The second column of Table 3 and Figure 6b show a big family of peaks. The peaks are multiples of the first fundamental frequency $\omega_1=1769$ Hz (the control value $\alpha=10$). The multiple multipliers are $m_1=2, m_2=3, m_3=4, m_4=5, m_5=6$,…, $m_{10}=11$.

Further, increasing the control parameter up to $\alpha=11.5$ produces more peaks (Figure 6c), especially in the low-frequency domain. The frequency 1561 Hz appears on the place where earlier has been the spectral "trough". It can be seen that increasing the value of the control parameter from $\alpha=10$ to $\alpha=11.5$ leads to halve of the fundamental frequency 1561 Hz a number of times. Peaks at 409.5 Hz, 767.6 Hz, 1177 Hz have appeared, which is entirely consistent with the well-known “period doubling” scenario ($T_1=\frac{2\pi}{\omega_1}\rightarrow 2T_1=\frac{2\pi}{\omega_1/2}$) [20].

The frequencies of the peaks are multiples ($m_1 = 2, m_2 = 3, ..., m_{10} = 11$) of the fundamental frequency $\omega_1 = 409.5$ Hz. The peak near the frequency 1792 Hz presents too, but in comparison with the previous case, when the peak has been observed at 1769 Hz, the magnitude significantly has reduced from -33.65 dB to -44.01 dB.

Finally, when $\alpha = 12.3$ the first fundamental frequency $\omega_1 = 409.5$ Hz halves again and becomes $\omega_1 = 196$ Hz. The relative height of former spectral peaks (on the frequencies that are multiples to the frequency 409.5 Hz) decreases in comparison with a common background of the power spectrum (Fig. 6d). It has happened because new modes appeared with the harmonics which are multiples of the second fundamental frequency $\omega_2 = 710.5$ Hz (for instance, with the multiplier $m_2 = 3$, corresponds to the new frequency 2107 Hz).

Thus, in the case $\alpha = 12.3$ the energy redistribution in the power spectrum of a quasi-periodic signal with two periods occurs. The redistribution process includes energy outflow from spectral modes with the multiple harmonics to the first fundamental frequency $\omega_1 = 196$ Hz (the "former" first $\omega_1 = 409.5$ Hz). It also leads to decreasing of the mode's amplitudes (Fig. 6d) due to energy inflow to the spectral modes with harmonics that are multiples of the second fundamental frequency $\omega_2 = 710.5$ Hz.

As already noted, at the ratio $\omega_2 / \omega_1 = 3.625$ the power spectrum of such a quasi-periodic signal ($\alpha = 12.3$) becomes rather dense, but not continuous.

Further, increasing the control value to $\alpha = 13.5$ leads to appear third fundamental frequency $\omega_3 = 447.7$ Hz (Fig. 6, e) in the low-frequency area of the spectrum. In turn, it leads to gradual alignment (smoothing) of the already existing spectral modes in amplitude due to the appearance of the new modes that are multiples of the ω_3 . The RTN theory predicts the Hopf's supercritical third bifurcation generating a transition from a quasiperiodic state with two frequencies to a quasiperiodic state with three frequencies [19]. The scenario is entirely consistent with the computational experiments described above.

When the value $\alpha = 14$, amplification in the low-frequency area of the spectrum near the third fundamental frequency occurs as well as resonant harmonics is damping. (Fig. 6f). Thus, the spectrum becomes similar to the spectrum of an aperiodic signal, i.e. almost continuous. It means that when $\alpha > 14$ (in particular case, $\alpha = 15.6$) the chaotic regime in the state-space of Chua's circuit can be observed (Fig. 8).

Let us note that if the control parameter decreases from $\alpha = 14$ to $\alpha = 11.5$, the harmonics which are multiple to the fundamental frequencies ω_2 and ω_3 begin

to disappear due to synchronization between ω_1, ω_2 and ω_3 (the phenomenon of frequency pulling) [20].

In this case, if the value of α decreases the frequencies ω_2 and ω_3 gradually increase, so that the ratio, for example ω_2 / ω_3, becomes a rational number. It means that $\omega_2 / \omega_3 = n_2 / n_3$ where n_2, n_3 are integers. Consequently, the quasi-periodic signal can become the periodic one with a period $\mathrm{T}_1 = n_2 \mathrm{T}_2 = n_3 \mathrm{T}_3$. Really, according to (14) we can see that

$$x(\omega_1 t, \omega_2 t, \omega_3 t) = x(\omega_1 t + 2\pi n_1, \omega_2 t + 2\pi n_2, \omega_3 t + 2\pi n_3). \tag{18}$$

When frequency synchronization occurs: $\omega_2 / n_2 = \omega_3 / n_3$, then all lines of the power spectrum are modes with harmonics of the lowest frequency

$$\omega_1 = \frac{\omega_2}{n_2} = \frac{\omega_3}{n_3}. \tag{19}$$

Substituting (19) in (18) we obtain that quasiperiodic signal becomes periodic one:

$$x(\omega_1 t, \omega_2 t, \omega_3 t) = x(\omega_1 t + 2\pi n_1, \omega_1 n_2 t + 2\pi n_2, \omega_1 n_3 t + 2\pi n_3) \equiv \breve{x}(\omega_1 t) \tag{20}$$

so that the neighbouring lines of the power spectrum are always separated by the same distance $2\pi / \mathrm{T}_1$ (see, for example, Fig. 9a).

3 Conclusion

This work describes the application of the method of matrix decomposition developed by A.M. Krot for analysis of Chua's chaotic generator. The method is based on the decomposition of vector function in Taylor multiple series. It can be also used for analyzing other electronic circuits being in chaotic regimes. This approach allows us to split up the original operator of the system of differential equations into linear, quadratic and cubic terms with the aim to estimate the contribution of each term in whole dynamics of Chua's circuit. It develops the process of circuit analysis by obtaining new data that could not be extracted using traditional Chua's circuit [22]. In particular, it allows us estimating the influence of high-order nonlinearities based on the described kernels $L^{(1)}_{N\times N}$, $L^{(2)}_{N\times N^2}$, $L^{(3)}_{N\times N^3}$.

The investigation shows that the process of occurrence of chaotic oscillations in the Chua's circuit corresponds to Landau's model of initial turbulence in full accordance with the theory of Ruelle-Takens. Unlike Landau's model, the new set of stationary values u_1^* that provides chaotic dynamics of the circuit has been introduced. Combining the control parameters, including the stationary value u_1^*, the double-scroll attractor has been obtained. Using bifurcation and spectral analysis, a mechanism of the chaotic regime appearance has been investigated.

Acknowledgements

This work has been supported partially by the grant of President of the Republic of Belarus in science (2019) and Swiss State Secretariat for Education, Research and Innovation (SERI) grant SFG 450 “Neuromorphic controller for an autonomous robotic vehicle” (24.09.2018).

References

1. G. Tanaka, T. Yamane, J.B. Héroux, R. Nakane, N. Kanazawa, S. Takeda, H. Numata, D. Nakano, A. Hirose. Recent Advances in Physical Reservoir Computing: A Review. *Neural networks : the official journal of the International Neural Network Society*, 115, 100-123, 2019.
2. A.M. Krot. Chaotic dynamic methods based on decomposition of vector functions in vector-matrix series into state-space. *Melecon 2000: Proc. 10th Mediterranean Electrotechnical Conference*, 2:643–646, 2000.
3. A.M. Krot. The decomposition of vector functions in vector-matrix series into state-space of nonlinear dynamic system. *EUSIPCO-2000 : Proc. X European Signal Processing Conference*, 3:2453–2456, 2000.
4. A.M. Krot. Matrix decompositions of vector functions and shift operators on the trajectories of a nonlinear dynamical system. *Nonlinear Phenomena in Complex Systems*. Vol. 4, №2, 106–115, 2001.
5. A.M. Krot. Application of expansion into matrix to analysis of attractors of complex nonlinear dynamical systems. *DSP-2002 : Proc. 14th IEEE International Conference on Digital Signal Processing*. pp. 959–962, 2002.
6. A.M. Krot, H.B. Minervina. Minimal attractor embedding estimation based on matrix decomposition for analysis of dynamical systems. *Nonlinear Phenomena in Complex Systems*, Vol. 5, № 2. – P. 161–172, 2002.
7. A.M. Krot. The development of matrix decomposition theory for nonlinear analysis of chaotic attractors of complex systems and signals. *DSP-2009: Proc. 16th IEEE International Conference on Digital Signal Processing*, 1-5, 2009.
8. A.M. Krot. Bifurcation analysis of attractors of complex systems based on matrix decomposition theory. *IEM 2011: Proc. of IEEE Intern. Conference on Industrial Engineering and Management*, 1-5, 2011.
9. A.M. Krot. Nonlinear analysis of the Hopfield network dynamical states using matrix decomposition theory. *Chaotic modeling and simulation*, Vol. 1, pp. 133-146, 2013.
10. T. Matsumoto. Chaos in electronic circuits. *Proceedings of the IEEE.* Vol.75, *3*:1033-1057, 1987.

11. M. Ogorzalek, Z. Galias, L. Chua. Exploring chaos in Chua's circuit via unstable periodic orbits. *Circuits and Systems, ISCAS '93, IEEE International Symposium on*. pp. 2608-2611, 1993.
12. G. Zhong. Implementation of Chua's circuit with a cubic nonlinearity. *IEEE Transactions on Circuits and Systems*, Vol. 41, 12: pp. 934-941.
13. Z. Galias. Rigorous analysis of Chua's circuit with a smooth nonlinearity. *IEEE Transactions on Circuits and Systems I: Regular Papers*, Vol. 63, 12:2304-2312, 2016.
14. K. O'Donoghue, M.P. Kennedy, P. Forbes. A fast and simple implementation of Chua's oscillator using a "cubic-like" Chua diode. *Proceedings of the 2005 European Conference on Circuit Theory and Design, 2*, II/83-II/86, *2005*.
15. B. Srisuchinwong, Wimol San-um. Implementation of Chua's Chaotic Oscillator Using "Roughly-Cubic-Like" Nonlinearity. *4th International Conference on Electrical Engineering/Electronics, Computer, Telecommunications and Information Technology*, pp. 36-37, 2007.
16. Z. Galias. On the existence of chaos in the Chua's circuit with a smooth nonlinearity. *Circuits and Systems (ISCAS), IEEE*, pp. 1106-1109, 2016.
17. L. D. Landau, E. M. Lifshitz. Fluid Mechanics (translated by J. B. Sykes and W. H. Reid from original Russian published in 1944), *Pergamon Press*, Oxford, 1959.
18. D. Ruelle, F. Takens. On the nature of turbulence. *Communications in Mathematical Physics*, No. 21, pp. 167–192, 1971.
19. D. Ruelle, F. Takens, S. Newhouse. Occurrence of strange axiom A attractors near quasi periodic flows on T, $m \geq 3$. *Communications in Mathematical Physics*, No. 64, pp. 35–40, 1978.
20. P. Bergé, Y. Pomeau, C. Vidal. L'ordre dans le chaos: vers une approche déterministe de la turbulence. Hermann, Paris, 353 p., 1988.
21. F. Moon. Chaotic Vibrations: An Introduction for Applied Scientists and Engineers, John Wiley&Son, 309 p., 2004.
22. V. Siderskiy, A. Mohammed, V. Kapila. Chua's Circuit for Experimenters Using Readily Available Parts from a Hobby Electronics Store, *122nd ASEE Annual Conference & Exposition / WA*, Seattle : American Society for Engineering Education, 2015.